

Circulation Research

JOURNAL OF THE AMERICAN HEART ASSOCIATION



Vasomotor control of capillary transit time heterogeneity in the canine coronary circulation.

C P Rose and C A Goresky

Circ Res. 1976;39:541-554

doi: 10.1161/01.RES.39.4.541

Circulation Research is published by the American Heart Association, 7272 Greenville Avenue, Dallas, TX 75231

Copyright © 1976 American Heart Association, Inc. All rights reserved.

Print ISSN: 0009-7330. Online ISSN: 1524-4571

The online version of this article, along with updated information and services, is located on the World Wide Web at:

<http://circres.ahajournals.org/content/39/4/541>

Permissions: Requests for permissions to reproduce figures, tables, or portions of articles originally published in *Circulation Research* can be obtained via RightsLink, a service of the Copyright Clearance Center, not the Editorial Office. Once the online version of the published article for which permission is being requested is located, click Request Permissions in the middle column of the Web page under Services. Further information about this process is available in the [Permissions and Rights Question and Answer](#) document.

Reprints: Information about reprints can be found online at:
<http://www.lww.com/reprints>

Subscriptions: Information about subscribing to *Circulation Research* is online at:
<http://circres.ahajournals.org/subscriptions/>

12. Rudolph AM, Yuan S: Response of the pulmonary vasculature to hypoxia and H^+ ion concentration changes. *J Clin Invest* 45: 399-411, 1966
13. Campbell AGM, Dawes GS, Fishman AP, Hyman AI: Pulmonary vasoconstriction and changes in heart rate during asphyxia in immature fetal lambs. *J Physiol (Lond)* 192: 93, 1967
14. Comline RS, Silver M: The release of adrenaline and noradrenaline from the adrenal glands in the fetal sheep. *J Physiol (Lond)* 156: 424-444, 1961
15. Wagenvoort CA, Neufeld HN, Edwards JE: The structure of the pulmonary arterial tree in fetal and early postnatal life. *Lab Invest* 10: 751-762, 1961
16. Naeye RL: Arterial changes during the perinatal period. *Arch Pathol* 71: 121-128, 1961
17. Levin DL, Rudolph AM, Heymann MA, Phibbs RH: Morphological development of the pulmonary vascular bed in fetal lambs. *Circulation* 53: 144-151, 1976

Vasomotor Control of Capillary Transit Time Heterogeneity in the Canine Coronary Circulation

COLIN P. ROSE, M.D., AND CARL A. GORESKY, M.D., PH.D.

SUMMARY A set of indicator-dilution studies of the coronary circulation of the intact functioning heart was carried out in the dog to provide a data base for defining the effect of changes in vasomotor control on the exchange of materials across the myocardial capillaries. The reference substance used was ^{125}I -labeled albumin; the diffusible substance used was ^{14}C -labeled sucrose. Model analyses of the data were carried out. In previous models of the capillary exchange in the coronary circulation, it had been assumed that a single capillary transit time is representative of the whole. **The data**

acquired here indicate that there is a very large heterogeneity of capillary transit times in the intact heart, and that the single transit time model is approximately true only when the resistance vessels are maximally dilated. The present pattern of findings is explained best by a model of the coronary microcirculation based on capillary-large vessel units with a variable heterogeneity of flow or capillary lengths, hence of transit times. We conclude that a major determinant of the extraction of each diffusible substance, on a microscopic level, is the distribution of capillary transit times.

INDICATOR-DILUTION studies of the coronary circulation will contain information especially concerning the heterogeneity of capillary transit times, information which potentially can be resolved from outflow curves if both a vascular reference substance, one confined to the coronary circulation, and a diffusible substance, one which leaves the vascular space, have been injected simultaneously. One would expect the heterogeneity to change with changes in the vasomotor tone, and this change, in turn, to affect the manner of presentation of diffusible substrates to muscle cells, where they are utilized. It therefore seemed important to us to develop a way of characterizing the heterogeneity of capillary transit times in the myocardium and to use this to define the manner in which the heterogeneity alters in response to changes in vasomotor control.

The essence of this methodology is to carry out a set of indicator-dilution experiments, to develop a model of events at the level of the capillary net, and, with this, to try to dissect from the data information concerning the heterogeneity of capillary transit times.

Although the construction of mathematical models of the single capillary is relatively advanced,¹⁻³ it rarely has been possible to isolate a single capillary and its surrounding tissue. **The transport data available have been those from whole organs and are a summation of effects at the level of millions of capillaries, which may differ in their lengths, flow rates, and diffusional interactions.** In order to extract information on the intrinsic characteristics of transport by the capillary wall and tissue cells, the organ model must be extended to include this heterogeneity.

Goresky et al.³ previously have considered two models representing the extreme cases, i.e., no heterogeneity, and maximum heterogeneity in capillary transit times. **Multiple indicator-dilution data from the liver fit the latter model very well.**⁴ The data from the heart, on the other hand, have always been assumed to exhibit very little or no heterogeneity of capillary transit times and to represent the other extreme,⁵⁻⁷ although the matter really has not previously been tested.

In the present study we found, in the course of analyzing many multiple indicator-dilution experiments on the heart, that this assumption did not provide an adequate description of the data, that it approximated the data only when the coronary circulation was maximally dilated, and that in general there was evidence of a large degree of heterogeneity, which varied with the degree of coronary vascular resistance. To account for this, we developed a mathematical model of the coronary circulation based on capillary-large vessel units in which there is a heterogeneity of flow, hence of capillary transit times, and, with this, we then were

From the McGill University Medical Clinic in The Montreal General Hospital.

Supported by the Medical Research Council of Canada and the Quebec Heart Foundation.

Dr. Rose is a Fellow of the Canadian Heart Foundation, and Dr. Goresky is a Medical Research Associate of the Medical Research Council of Canada.

Presented in part at the annual meeting of the American Physiological Society, Anaheim, California, April 12, 1976.

Address for reprints: Dr. C.A. Goresky, University Medical Clinic, Montreal General Hospital, 1650 Cedar Avenue, Montreal, Quebec, Canada H3G 1A4.

Received October 15, 1975; accepted for publication June 8, 1976.

able to develop a method for determining a characteristic set of parameters which both describe the heterogeneity and characterize the exchange of diffusible substances in the intact heart. This analysis has provided an approach to the working linkage between changes in the coronary vascular resistance and changes at the level of the microvasculature, that is, to the functional architecture of the coronary circulation.

While we were considering the problem of heterogeneity from the point of view of tracer outflow, reports of two studies using the microsphere injection and tissue sampling technique appeared.^{8, 9} These demonstrated the presence of macroscopic flow heterogeneity, at the level of 1-g blocks of tissue, and complement the findings from the present study even though they are not directly comparable.

Methods

GENERAL EXPERIMENTAL PROCEDURE

The general experimental design is that of a multiple indicator-dilution experiment.¹⁰ Two substances are injected: ¹²⁵I-labeled albumin, a reference substance that does not leave the circulation within a single passage;⁶ and ¹⁴C-labeled sucrose, a diffusible substance that leaves the capillaries during its passage through the coronary circulation to enter the extracellular space. Multiple outflow samples then are collected.

EXPERIMENTAL PREPARATION

The chest of a mongrel dog anesthetized with pentobarbital (30 mg/kg, iv) and ventilated by a constant volume respirator was opened in the 4th left intercostal space, the pericardium was incised, and a catheter was manipulated into the coronary sinus via the right jugular vein. A pericardial cradle was constructed and the left main coronary artery or one of its branches was isolated. After the dog had been anticoagulated with heparin (3 mg/kg), the perfusion system, consisting of a heat exchanger, a peristaltic pump (Sigmamotor), and an air-filled damping chamber to obviate the pressure and flow transients which otherwise would result from a sudden injection,⁶ was primed with blood from the femoral artery and a cannula was inserted via a common carotid artery and tied into a previously isolated coronary artery. Another peristaltic pump was used to sample blood from the coronary sinus at a constant rate. The perfusion rate was adjusted to maintain the coronary sinus PO₂ at 20–30 torr. Aortic or left ventricular pressure was monitored by a catheter inserted via the other femoral artery. The electrocardiogram (ECG), perfusion pressure, and perfusion flow were monitored continuously, the latter by means of a Biotronix extracorporeal flowmeter. Intracoronary infusions of substances affecting vasomotor control were made into the perfusion tubing with a Harvard infusion pump.

Maximal vasodilation was assumed to have occurred when a transient reduction in flow resulted in no reactive hyperemic response.

INJECTION MIXTURE

We added 0.1 mCi of sucrose-¹⁴C(U) (New England Nuclear) and 0.05 mCi of ¹²⁵I-human albumin (Charles E.

Frosst) to 6 ml of blood. The mixture was adjusted to a final hematocrit identical to that of the dog.

EXPERIMENTAL PROTOCOL

When the preparation was in a steady state with respect to arterial pressure and coronary resistance, a sudden injection of 0.3–0.5 ml of the injection mixture was made into the perfusion tubing. Simultaneously, the collection rack was started and samples were collected at a rate of 0.5–0.8 sec/sample. Immediately after the run, samples were collected from the femoral artery and coronary sinus for determinations of blood gases and pH. Homologous blood was transfused as necessary to sustain arterial pressure.

Prior to removal of the cannula, a concentrated solution of T-1824 (Evans blue) was infused, to demarcate the portion of the heart perfused. The stained portion was excised and weighed. These weights are the values reported later. The cannula then was perfused alone, at the same rate as had been used during the experimental runs. The pressure required for this perfusion was subtracted to give the value reported later, a coronary artery pressure corrected for cannula effects.

The experiments reported here are part of a larger study concerning transport of metabolites in the coronary circulation. The effect of changes in vasomotor control on the interrelations of the two dilution curves was first observed after intracoronary infusions of either α -bromopalmitate or flavaspidic acid, substances that exert metabolically deleterious effects on the heart and consequently cause vasodilation. We later found that the same effect occurs with any stimulus causing vasodilation. In these experiments vasodilation was induced while the flow was held relatively constant. This results in a reduction in perfusion pressure. We thought that it was better to compare vasodilation at relatively constant flow rather than at constant pressure, since in the latter case the increased flow which occurs during vasodilation shortens the capillary transit times and reduces the extraction of diffusible tracer, so that the control and vasodilated runs are less comparable.

ANALYSIS OF SAMPLES

A volume of 0.1 ml of each sample was diluted in 1.5 ml of saline and pipetted into a test tube and assayed for radioactivity in a gamma ray spectrometer set for the photopeak characteristic of ¹²⁵I. The proteins then were precipitated with 0.2 ml of trichloroacetic acid, and 0.2 ml of the supernatant fluid was pipetted into a scintillation cocktail and assayed for ¹⁴C activity in a liquid scintillation counter. Samples from the injection mixture and crossover standards were treated identically. To normalize the activity resulting from each of the tracers, with respect to the other, the outflow activity of each was divided by the total activity injected, for that species. The resulting value is a fraction of the total injected per milliliter of venous blood.

STATIONARITY CONSIDERATIONS

Multiple indicator-dilution experiments usually are considered to yield valid data only in the situation in which the system is not changing as a function of time. For the situation considered here, the hemodynamic parameters are stable over periods which are large, compared to the

duration of the experiment, but the microsphere injection-tissue sampling experiments suggest that there is a background small scale temporal oscillation in spatial heterogeneity, with a long periodicity (of the order of 60 seconds), the whole operating in such a fashion that changes in one area are compensated for by those in another.^{8, 9} The result of this is that the whole becomes equivalent, in a statistical sense, to an unchanging stationary system.

The Biological Problem

CHANGES IN THE TRACER OUTFLOW CURVES AND IN INSTANTANEOUS EXTRACTIONS, WITH CHANGES IN CORONARY VASCULAR RESISTANCE

Typical sets of dilution curves, for a control and a very vasodilated state, are shown in Figure 1. In each instance loss of the permeating indicator, labeled sucrose, from the capillary bed results in a sucrose curve which is lower on the upslope and peak than the curve for the reference indicator, labeled albumin; and later, on the downslope, return of the extravascular tracer results in a sucrose curve which crosses that for labeled albumin. The areas under both curves are the same, when recirculation is excluded, and the data are accumulated for a period sufficiently long to inscribe complete dilution curves.⁶

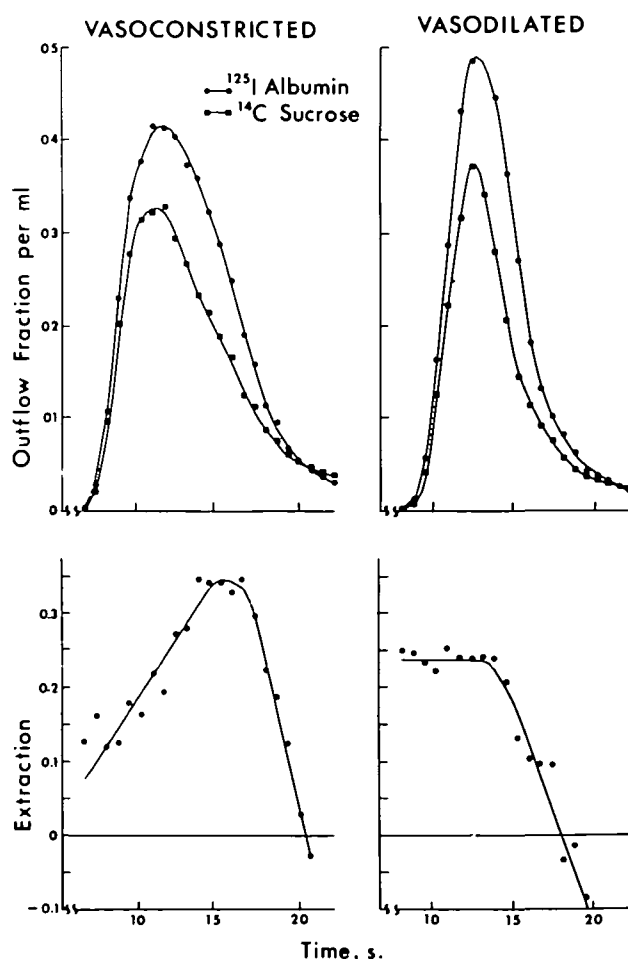


FIGURE 1 Upper panels: outflow curves for a typical experiment (no. 6 of Table 1); run 1, in the normal state, is on the left, and run 2, in the vasodilated state, is on the right. Lower panels: calculated "instantaneous extractions" for each run.

After vasodilation both curves show less dispersion, and the relation between the two curves changes. In the control run the sucrose curve tends to diverge progressively from the reference curve on the upslope, over the peak, and on the early downslope; whereas, after vasodilation, the sucrose curve appears to be a more or less constant fraction of the reference curve, on the upslope, up to the peak. A classic way to illustrate the relation between the reference and diffusible curves is the "instantaneous extraction," $E(t)$, defined by Crone,¹¹ $E(t) = 1 - [C(t)_{\text{sucrose}}/C(t)_{\text{albumin}}]$, where $C(t)$ is the appropriate outflow fraction per milliliter. This fraction is illustrated in the lower panels for the two runs of Figure 1. In the normal, relatively vasoconstricted coronary circulation, the early extractions increase by a factor of 2–3, to reach a maximum later in time than the peak of the albumin outflow curve. The extraction values thereafter rapidly decrease. In the vasodilated run, the extractions appear relatively constant, early in time, with no really apparent maximum; and, soon after the albumin peak, decrease rapidly.

The data illustrated in past publications^{5, 6, 12} have, in form, resembled the curves of the vasodilated run. The extractions have assumed relatively constant values on the upslope, to the peak, and then have decreased. The form is that expected if the capillary transit times are uniform, and the later decrease in extraction may be taken to signify the return of material from the extravascular space.^{1, 7} If there were no return the extractions would simply continue in a linear fashion.¹³ In the vasoconstricted run the data do not correspond to these preconceived notions and some new approach needs to be devised. If we use the same kind of logic here, and assume that tracer return begins when the extraction curve starts to decrease from its highest value, the form of the early part of the curve indicates that the extractions have increased progressively with time; and one could infer that, if the return of tracer did not occur, the pathways which emerge latest would have an even higher extraction.¹ In this case no single value for the extraction exists. The first intuitive explanation of such an increase in extraction with time is that capillary transit times corresponding to the various parts of the vascular reference outflow curve increase with time.

A general hypothesis is needed to explain the change in the pattern of extractions with change in the vascular resistance and it appears that this hypothesis must be one which obviates the necessity of always expecting a single value extraction.

The Evolution of a Model

We must now develop an appropriate model and evaluate its propriety by using it to analyze the indicator-dilution data acquired in the present experiments. In carrying out this task we first outline the impulse response of the single capillary and then develop a set of models incorporating this, which are characterized by the various patterns of distribution of capillary transit times which we might expect to encounter.

IMPULSE RESPONSE OF THE SINGLE CAPILLARY

The background considerations and details of a single capillary model appropriate to the heart have been explored,

in extenso, by Goresky et al.;¹ this, in turn, corresponds closely to that described by Bassingthwaite⁷ for the case in which longitudinal diffusion is too small to be of importance. The essence of the model, necessary to our further considerations, is described below.

Let u and v be the concentration of tracer in intravascular and extravascular spaces, respectively; W , the plasma bulk flow velocity in the capillary; x , the distance along the capillary; γ , the ratio of accessible extravascular to intravascular volume; and k_1 and k_2 the permeability-surface products for efflux from and influx into the capillary per volume of accessible extravascular space (these will be equal when the exchange is passive).

For conservation of matter

$$\frac{\partial u}{\partial t} + W \frac{\partial u}{\partial x} + \gamma \frac{\partial v}{\partial t} = 0, \quad (1)$$

and for the rate of accumulation with the extravascular space

$$\frac{\partial v}{\partial t} = k_1 u - k_2 v. \quad (2)$$

The simultaneous solution of the equations, for an impulse input, is

$$u(L, t) = \frac{q_0}{F_c} e^{-k_1 \gamma \tau_c} \delta(t - \tau_c) + \frac{q_0}{F_c} e^{-k_2 t} e^{-\tau_c(k_1 \gamma - k_2)} \sum_{n=1}^{\infty} \frac{(k_1 k_2 \gamma \tau_c)^n (t - \tau_c)^{n-1}}{n! (n-1)!} S(t - \tau_c) \quad (3)$$

where L is the length of the capillary, q_0 is the amount of tracer in the input, F_c is the flow in the capillary, and τ_c is the transit time of the capillary. $\delta(t - \tau_c)$ indicates a Dirac delta or unit impulse function delayed to $t = \tau_c$ and $S(t - \tau_c)$ a unit step function delayed at onset to $t = \tau_c$. It should be noted that the product $k_1 \gamma$ in the exponent of the damping factor of the first term is equal to the ratio of the capillary permeability-surface product PS_c to the capillary volume V_c accessible to the label (a plasma volume, if the label does not enter the red cells); and that τ_c in the exponent is the ratio of the accessible capillary volume to the appropriate flow. The exponent is thus equal to the ratio (permeability-surface product/flow).

IMPULSE RESPONSE OF THE HEART

The impulse response of the heart will be the summation of all of the effects of the single capillaries within the whole. The problem facing us is that of describing the manner in which the capillary and large vessel transit times are distributed, and hence the expected form of the output from the organ as a whole.

Our analysis will be discussed in terms of three models. The first two are the extremes previously described by Goresky et al.,¹ that with no heterogeneity of capillary transit times, and that with a "maximum" heterogeneity of capillary transit times (the latter case is considered to occur when essentially all of the dispersion of reference tracer occurs in the capillaries). The third is a more general model

which includes the first two models as limiting cases and, we believe, more closely approximates the transport characteristics of the coronary circulation.

All three models are based on the same fundamental assumptions: (1) the amount of tracer delivered to each capillary is proportional to the flow to it, and (2) diffusional interaction between capillaries can be neglected. This implies that the fundamental unit of the microcirculation is a bundle of similar capillaries, with apposed entrances and exits and equal flows. In this situation no *net* flux occurs across the interface.

Model 1. Constant Capillary Transit Time and Varying Large Vessel Transit Times

This model assumes that all of the dispersion of intravascular tracer is due to variation in large vessel transit times and that the capillary transit time is a constant and contributes only a uniform time delay to the intravascular distribution.

For the intravascular tracer the output concentration,

$$C(t)_{ref} = \frac{q}{F} r(t - \tau_c) = \frac{q}{F} r(\tau_1) \quad (4)$$

where $r(\tau_1)$ is the distribution of large vessel transit times, τ_c is the common capillary transit time, q is the total amount of tracer injected, and F is the total flow.

For the exchanging diffusible tracer

$$C(t)_{diff} = \frac{q}{F} e^{-k_1 \gamma \tau_c} r(t - \tau_c) + \frac{q}{F} e^{-k_1 \gamma \tau_c} \int_{\tau_{1m}}^{t - \tau_c} e^{-k_2(t - \tau_c - s)} r(s) \cdot \sum_{n=1}^{\infty} \frac{(k_1 \gamma k_2 \tau_c)^n (t - \tau_c - s)^{n-1}}{n! (n-1)!} ds \quad (5)$$

where τ_{1m} is the minimum large vessel transit time.

Ziegler and Goresky^{6, 13} used this model in the analysis of their dilution data for sodium, sulfate, and rubidium ions, and sucrose in the heart. In these papers the reciprocal of the product of γ and τ_c was developed as a single parameter, Φ , the flow per volume of accessible extravascular space. The reason for doing this was not stated explicitly but becomes evident when one begins to use this model to fit experimental data. When an attempt is made to use the data to optimize numerical estimates of the parameters, the fitting process is found to provide a constant estimate of the product $\gamma \tau_c$ rather than constant values for the individual parameters γ and τ_c . The estimates of γ and τ_c thus are found to vary reciprocally. In fitting this model to coronary venous dilution curves, obtained in a working heart in situ, Ziegler and Goresky⁶ also found that the fit provided a constant and systematic underestimate of the experimental values on the upslope of the curve for the diffusible reference. They attributed this finding to the outflow, early in time, of capillaries with transit times shorter than the average (that is, to a set of phenomena not included in this particular modeling). The solution to the problem was not undertaken.

Model II. Constant Large Vessel Transit Time and Varying Capillary Transit Times

This model is the converse of model I. It assumes that all of the intravascular tracer dispersion occurs within the capillaries, a maximum heterogeneity. For the reference tracer

$$C(t)_{\text{ref}} = \frac{q}{F} n(t - \tau_1) = \frac{q}{F} n(\tau_c) \quad (6)$$

where $n(\tau_c)$ is the distribution of capillary transit times, and τ_1 is the common large vessel transit time.

For the diffusible tracer

$$C(t)_{\text{diff}} = \frac{q}{F} e^{-k_1 \gamma (t - \tau_1)} n(t - \tau_1) + \frac{q}{F} e^{-k_2 (t - \tau_1)} \int_{\tau_{cm}}^{t - \tau_1} e^{-s(k_1 \gamma - k_2)} n(s) \cdot \sum_{n=1}^{\infty} \frac{(k_1 \gamma k_2 s)^n (t - \tau_1 - s)^{n-1}}{n!(n-1)!} ds \quad (7)$$

where τ_{cm} is the minimum capillary transit time.

This is the model which, in its flow-limited extreme, Goresky⁴ has used to fit data from the liver. It allows independent optimization of γ because τ_{cm} is defined implicitly as being equal to the time after a common large vessel transit time.

Model III. Varying Capillary and Large Vessel Transit Times: The Parallel Capillary-Large Vessel Unit Model

While there are potentially an infinite number of combinations of capillary and large vessel transit times that will generate the dispersion of the intravascular reference, the information contained in the dispersions of the diffusible and sequestered tracers is theoretically adequate to allow a selection of the correct combination, if its form can be guessed. A few clues derived from the dilution data result in a model which, we think, is a close approximation to the partition of capillary and large vessel times characteristic of the coronary circulation.

It became apparent, on initial attempts at analysis, that even in the same heart, different sets of dilution curves, recorded under conditions of varying vasomotor control, possess differing combinations of capillary and large vessel transit times and that any model would have to be individualized to each experiment. The variation seems to be related to the response of the coronary circulation to both endogenous and exogenous stimuli. Figure 2 illustrates the kind of variation encountered. Two sets of data from the same heart are depicted—the “normal” set obtained while the heart was generating 110 mm Hg systolic pressure, and the “fibrillating” set, just after the heart had been maximally dilated and fibrillated. In each instance the logarithm of the ratio of the outflow fraction per milliliter for the reference substance to that for the diffusible substance is plotted against time (this is the “natural kind of plot” which arises from the relation between the first or throughput parts of the two curves). For each run the initial segment of the plot is a straight line; and this is then succeeded by a later part, which deviates sharply downward, as a significant amount of

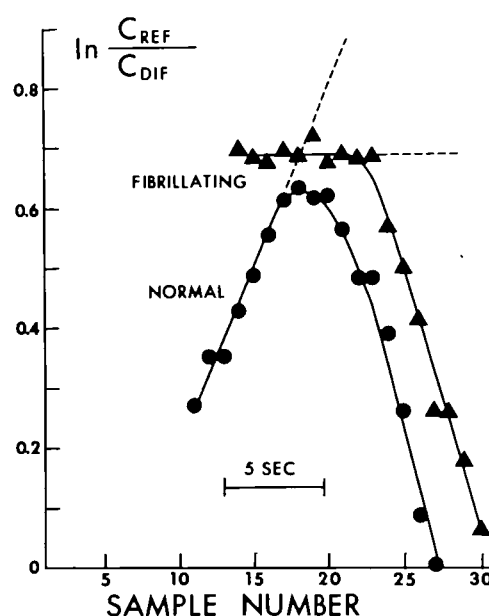


FIGURE 2 Log-ratio time plots from the same heart in the “normal” or relatively vasoconstricted state of the coronary circulation (●) and in the vasodilated and fibrillating state (▲). $C_{\text{ref}}/C_{\text{diff}}$ is the ratio of normalized outflow concentrations of albumin (the reference) to that of sucrose (the diffusible tracer). The initial linear part of the curves before significant return from the extravascular space has been extrapolated (dashed lines) to emphasize that in the normal case the ratio would be expected to increase progressively, in the absence of returning tracer. The values presented correspond to runs 1 and 2 of experiment 1 in Table 1. These initial slopes, estimated by eye, do not necessarily represent the best slope obtained from the fitting procedure.

material returns from the extravascular space. In the fibrillating heart, with a maximally dilated coronary circulation, the slope of the initial line segment is small, whereas in the heart with a relatively constricted coronary circulation, a substantial positive slope is obtained. Partially vasodilated preparations yield an intermediate value for the slope. The maximally dilated heart thus results in a plot which represents an extreme in the family of curves obtained.

If we assume that the capillary transit time $\tau_c(t)$ is a function of time, then from the foregoing modeling we would expect, for the samples early in time,

$$\ln \left[\frac{C(t)_{\text{ref}}}{C(t)_{\text{diff}}} \right] = k_1 \gamma \tau_c(t). \quad (8)$$

For the fibrillating maximally vasodilated heart $\tau_c(t)$ must be almost a constant, if we assume that $k_1 \gamma$ is constant. In the “normal” experiment, in contrast, the function $k_1 \gamma \tau_c(t)$ increases with time. If we examine this function at a given time τ_c , we find that

$$k_1 \gamma \tau_c = P(S_c/V_c)(V_c/F_c).$$

Within this expression we would expect P to be relatively constant, (S_c/V_c) to be an architectural constant, and (V_c/F_c) to be a variable, depending on the flow. Thus we would expect the increase in $\tau_c(t)$ with time to be the result of the progressive outflow from capillaries which have longer and longer transit times. The time at the outflow, for each element, must have been partitioned between the large

vessels and the capillaries (since the sum of the two, for each element, equals the time of the outflow). We must therefore develop a time-partition function which contains a set of parameters which alter as the functional state of the coronary circulation changes.

To arrive at the required model we must find some way of relating the capillary transit time distribution to the distribution of large vessels. After trying various alternatives we found that, if we assumed that each set of identical capillary transit times was associated with a unique large vessel transit time such that progressively longer capillary transit times are associated with progressively longer large vessel transit times, we could obtain a satisfactory fit to the experimental data. Physically, this relation can exist if there is flow coupling between the set of capillaries and its feeding arteriole and draining venule. This implies that a group of capillaries fed by the same arteriole is also drained by a single venule; that is, if flow in the capillaries is slow, then that in the large vessels is slow, and so on. This assumption is really a corollary of the finding that the outflow capillary transit time is a linear function of time. It will be further amplified in later discussion.

If a' is the intercept at the appearance time of a straight line through the initial part of the log ratio-time plot and b' is its slope, then from Equation 8

$$k_1 \gamma \tau_c(t) = a' + b'(t - \tau_{cm} - \tau_{lm}) \quad (9)$$

where τ_{cm} is the minimum capillary transit time and τ_{lm} is the minimum large vessel transit time.

Now, for each capillary, $k_1 \gamma = PS_c / [\text{vascular space}]$ where PS_c is the permeability-surface product for that capillary. For albumin and sucrose the vascular space is $[1 - \text{capillary hematocrit}] \times [\text{capillary volume}]$. The parameter $k_1 \gamma$ is thus independent of capillary length at any hematocrit, providing permeability is constant along the length and must be, for the present purposes, regarded as constant.

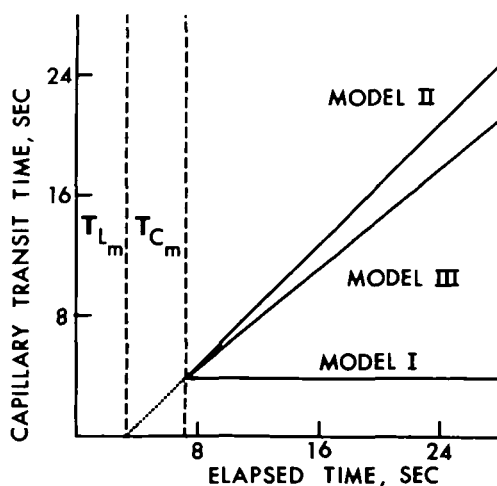


FIGURE 3 Relationship between the three models. For models I and III the minimum transit time is indeterminate but is made equal to that for model II for purposes of comparison. The slope of the line for model III can assume any value between those for the other two models, depending upon the degree of vasodilation of the preparation. The parameters T_{Lm} and T_{Cm} represent hypothetical minimum transit times for the large vessels and capillaries, respectively.

Therefore,

$$\tau_c(t) = a + b(t - \tau_{lm} - \tau_{cm}) \quad (9A)$$

where $a = \tau_{cm}$; and

$$\tau_l(t) = \tau_{lm} + (1 - b)(t - \tau_{lm} - \tau_{cm}). \quad (9B)$$

If $w[\tau_c(t) + \tau_l(t)]dt$ is the number of capillary-large vessel units with total transit times between $[\tau_c(t) + \tau_l(t)]$ and $[\tau_c(t) + \tau_l(t) + dt]$,

$$C(t) = \frac{q}{F} \int_{\tau_{cm} + \tau_{lm}}^t \frac{F_0}{Q_0} u[L, t - \tau_l(s)] \cdot w[\tau_c(s) + \tau_l(s)] ds. \quad (10)$$

For the intravascular reference,

$$C(t)_{ref} = \frac{q}{F} w[\tau_c(t) + \tau_l(t)], \quad (11)$$

and for the diffusible tracer,

$$C(t)_{diff} = \frac{q}{F} e^{-k_1 \gamma \tau_c(t)} w[\tau_c(t) + \tau_l(t)] + \frac{q}{F} \int_{\tau_{cm} + \tau_{lm}}^t e^{-k_2 [t - \tau_l(s)]} w[\tau_c(s) + \tau_l(s)] e^{-\tau_c(s) [k_1 \gamma - k_2]} \times \sum_{n=1}^{\infty} \frac{[k_1 \gamma k_2 \tau_c(s)]^n [t - \tau_c(s) - \tau_l(s)]^{n-1} ds}{n!(n-1)!}. \quad (12)$$

Just as with model I, only the product of $\tau_c(t)$ and γ is determinable and it is necessary to have an independent measure of either γ or $\tau_c(t)$ at some time, to obtain the other.

Figure 3 shows the relation between the three models. The value for the minimum capillary transit time is arbitrary for models I and III and is made equal to that for model II for purposes of illustration. The crucial difference between the models is the change of the partitioning of the elapsed time between capillaries and large vessels. In general, for model III

$$\frac{\tau_c(t)}{\tau_l(t)} = \frac{\tau_{cm} + b(t - \tau_{cm} - \tau_{lm})}{\tau_{lm} + (1 - b)(t - \tau_{cm} - \tau_{lm})}, \quad t \geq \tau_{cm} + \tau_{lm}.$$

When $b = 0$, the expression collapses to that corresponding to model I, the constant capillary transit time model

$$\frac{\tau_c(t)}{\tau_l(t)} = \frac{\tau_{cm}}{t - \tau_{cm}}$$

And when $b = 1$, the expression collapses to that corresponding to model II, the constant large vessel transit time model

$$\frac{\tau_c(t)}{\tau_l(t)} = \frac{t - \tau_{lm}}{\tau_{lm}}.$$

THE FLOW-LIMITED CASE

For a single capillary the delayed wave flow-limited output is given by

$$u(L, t) = \frac{Q_0}{F_c} \delta[t - (1 + \gamma)\tau] \quad (13)$$

For the whole organ we find, for model III,

$$\begin{aligned} C(t)_{diff} &= \frac{q}{F} \int_{\tau_{cm} + \tau_{lm}}^t \delta[t - \tau_1(s) - (1 + \gamma)\tau_o(s)] \\ &\quad \cdot w[\tau_1(s) + \tau_o(s)] ds \\ &= \frac{q}{F} \int_{\tau_{cm} + \tau_{lm}}^t \delta[t - s(1 + b\gamma) \\ &\quad + \tau_{cm}\gamma(b - 1) + \tau_{lm}b\gamma] w[s] ds \\ &= \frac{q}{F} \frac{w\left\{\frac{t + (\tau_{cm} + \tau_{lm})b - \tau_{cm}}{1 + b\gamma}\right\}}{1 + b\gamma} \end{aligned} \quad (14)$$

When $b = 0$ (this corresponds to model I, where the capillary transit time becomes a constant τ_c), we find

$$C(t)_{diff} = \frac{q}{F} w(t - \gamma\tau_c). \quad (15)$$

In the original development of model I, the expression corresponding precisely to this would have been $(q/F)r[t - (1 + \gamma)\tau_c]$. The apparent discrepancy is due to the selection of the differing lower limit on the integral in Equation 14.

When $b = 1$ (this corresponds to model II, where the large vessel transit time becomes a constant τ_1), we find

$$C(t)_{diff} = \frac{q}{F} \frac{w\left\{\frac{t + \gamma\tau_1}{1 + \gamma}\right\}}{1 + \gamma} \quad (16)$$

Again, this corresponds precisely to the expression which results from model II, in the flow-limited case, $(q/F)n[(t - \tau_1)/(1 + \gamma)]/(1 + \gamma)$. Again the apparent discrepancy is due to the selection of the differing lower limit on the integral.

The presence of τ_{lm} in these formulas contributes only a uniform time delay which could be eliminated by selecting the appropriate zero time for the reference tracer. It is included in the general formulation chiefly to emphasize the fundamental distinctions between the models.

THE USE OF THE THREE MODELS TO DETERMINE INTRINSIC PARAMETERS FROM DATA

Neither model I nor model III permits absolute estimation of the minimum capillary transit time or γ , but model II allows absolute estimation of τ_{cm} and γ .

For the sucrose data analyzed here it is assumed that $k_1 = k_2 = k_s$, since there is no reason to think that the permeability properties of the interendothelial spaces are directional. The constant k_s is, then, the permeability-surface product per unit of accessible extravascular space for sucrose. If we can assume that the total space accessible to sucrose remains constant, independent of the number of capillaries open, and that the permeability of the capillaries is independent of perfusion pressure or flow rate, in the physiological range, then k_s is proportional to the number of open capillaries per unit volume of tissue.

γ , the ratio of accessible extravascular to intravascular spaces, can be separated in a fashion independent of other variables when using model II, the constant large vessel transit time model. Similarly, the parameter τ_{cm} is found to

be meaningful only with this model. For model I, the constant capillary transit time model, the parameter containing γ which can be optimized is $1/\gamma\tau_c$. This is equal to Φ , the flow per unit of accessible extravascular space. Φ can be calculated for the other models from the following formula

$$\Phi = \sum_{i=1}^n w_i \frac{1}{\gamma\tau_{c_i}},$$

where Φ in this case is a weighted average of the Φ 's for each capillary-large vessel unit, w_i is the weighting function obtained from the reference curve with the area normalized to one, and τ_{c_i} is the transit time corresponding to w_i .

It should be noted that, where we report a single value for k_s and γ , as a result of model analysis, we are also implicitly assuming that the capillary density is homogeneous and independent of the transit time, for a given state.

When fitting model III to data it is also necessary to determine the parameters a' and b' , which are a measure of the dispersion of transit times. A good guess to the best values for these parameters usually can be made by fitting a straight line by eye through the initial part of the log-ratio time curve. This guess then can be used as a starting point in the automatic fitting procedure. In contrast to k_s and F , a' and b' are an index of the structure of the microcirculation. A change in these parameters represents a change in the flow patterns in the microcirculation. Unfortunately, without knowledge of the absolute values for $\tau_c(t)$ or γ , the derived values for a or τ_{cm} and for b (the incremental change in capillary transit time with time) cannot be compared from one experiment to another.

In what follows, all three models are fitted to our experimental data. The appropriate parameters (depending on the model) are optimized so that the model corresponds as closely as possible to the data for the diffusible tracer (sucrose). The data, in this case, correspond to a barrier-limited kind of behavior, and the whole organ model, in each case, contains an integral containing the weighting function [$w(t)$, in model III; $r(t)$, in model I; and $n(t)$, in model II]. In order to obtain a good fit, a procedure to interpolate between the data points of the reference tracer is required. We have found that the most convenient and reliable method to do this is to fit a cubic spline through the data points and use the spline coefficients as required. Optimization of the fit to the diffusible tracer curve (by a steepest descent technique) is then carried out through a Fortran IV program, run from a remote terminal connected to an IBM 360 computer. In each case the program was allowed to run until there was no change in the third significant figure of any parameter. It usually required about 3–4 minutes of central processing unit (CPU) time per experiment.

CRITERION FOR GOODNESS OF FIT

The classic criterion for the goodness of fit is the coefficient of variation. We have found, however, that large changes in the fitted parameters can yield only small changes in the coefficient of variation. This is due to the lack of sensitivity of the parameters to the data that are less than 20% or 30% of the peak. In order to provide a criterion more sensitive to the lower data points, we have used the

coefficient of variation based on the logarithm of the outflow concentrations. Thus we have used the definition

$$\text{Coefficient of variation} = \frac{\sqrt{\frac{\sum_{i=1}^n [\log c_{o_i} - \log c_e]^2}{n-1}}}{(1/n) \sum_{i=1}^n \log c_{o_i}}$$

where n is the total number of data points, c_o is the observed value, and c_e is the estimated value.

Results

Table 1 presents the physiological data for the experiments analyzed. Experiment 1 was the first experiment in which the vasomotor effects were observed. Since, in run 2, the heart was fibrillating we originally thought that the change in the form of the dilution curves was due to the absence of a transmural pressure gradient. Further experiments, however, showed that essentially the same change in the form of the dilution curves occurred with vasodilation in the presence of a normal intraventricular pressure (experiments 4, 6, 7, and 8). Experiment 2 is included to demonstrate that two consecutive runs with no significant change in resistance give the same type of fits to the models. The absolute values for resistance are not comparable from one experiment to another.

Table 2 presents the results of fitting the three models to sets of data from representative experiments. In some

experiments there are two runs for the same heart and, in these instances, coronary vasodilation usually has been induced during the second run. Generally, model I (constant capillary transit times) gave poor fits in the intact hearts, but fitted quite well when vasodilation was induced. Model II (constant large vessel transit times) gave good fits in the intact hearts but resulted in parameter values that were physically impossible, in a large proportion of the vasodilated runs. Model III (variable capillary and large vessel transit times) in contrast, fitted all cases quite well, with no systematic deviations.

Figure 4 shows the actual data and model fits for the two runs of the first experiment in Table 2 (the numerical data underlying the continuous data curves in this illustration are presented in Table 3). The data were obtained first, with the heart in its normal state, and then, in the vasodilated, fibrillating state. The log-ratio curves illustrated in Figure 2 were derived from these data. Model III fits both sets of data better than do the other two models. In this illustration, one salient feature of the modeling immediately becomes evident, on visual inspection. It is that the throughput or first component of model I, the constant capillary transit time model, is constrained to be a constant fraction of the reference curve. This is the reason it necessarily fits the upslopes of curves from the vasoconstricted heart poorly.

In Table 2 we have reported the values for γ and τ_{cm} derived by fitting model II (the constant large vessel transit time model) to all experiments. In the experiments on the nonvasodilated hearts, where this asymptotic model fits

TABLE 1 Hemodynamic Parameters

Exp	Run	Perfused heart wt (g)	Flow ml/min	Hematocrit	Heart rate	Systolic pressure (torr)	Perfusion pressure (torr)	Resistance*	t_{alb}^\dagger (sec)
1	1	111	96	0.40	162	110	225	2.34	8.4
	2		67		0	0	45	0.67‡	9.5
2	1	112	87	0.25	144	115	248	2.85	7.7
	2		99		132	115	259	2.62	7.4
3	1	126	126	0.22	174	120	98	0.78	7.4
4	1	70	83	0.39	204	125	260	3.13	6.6
	2		83		204	115	130	1.57§	6.6
5	1	98	59	0.33	126	80	120	2.03	5.3
6	1	98	102	0.36	156	105	218	2.13	7.5
	2		119		138	75	64	0.54§	8.1
7	1	90	110	0.36	186	100	135	1.23	6.1
	2		122		192	90	68	0.55‡	6.0
8	1	—	82	0.35	132	125	65	0.79	8.9
	2		82		132	120	50	0.61‡	9.1
9	1	62	71	0.53	198	120	195	2.75	7.0
10	1	132	118	0.31	108	95	94	0.80	6.1

* Coronary resistance, torr ml⁻¹ min; the values have been corrected for cannula resistance.

† t_{alb} = mean transit time for albumin.

‡ Dilated by intracoronary infusion of flavaspidic acid; run 2 of experiment 1 also fibrillating.

§ Dilated by intracoronary infusion of α -bromopalmitate.

TABLE 2 *Derived Parameters for the Three Models*

Exp	Run	Model	k_s (sec ⁻¹)	Φ (sec ⁻¹)	γ	τ_{em} (sec)	c.v.*	a'	b' (sec ⁻¹)
1	1	I	0.0455	0.0828	—	—	0.0147	—	—
		II	0.0785	0.0979	1.22	1.73	0.00427	—	—
		III	0.0753	0.0942	—	—	0.00348	0.214	0.0866
	2	I	0.0558	0.0746	—	—	0.00368	—	—
		II	0.0634	0.0798	0.241	45.3†	0.00246	—	—
		III	0.0631	0.0767	—	—	0.00211	0.700	0.0161
2	1	I	0.0379	0.0921	—	—	0.00744	—	—
		II	0.0603	0.1220	1.11	2.36	0.00431	—	—
		III	0.0576	0.1160	—	—	0.00279	0.209	0.0555
	2	I	0.0324	0.133	—	—	0.00822	—	—
		II	0.0504	0.137	0.765	4.06	0.00438	—	—
		III	0.0519	0.131	—	—	0.00425	0.154	0.0405
3	1	I	0.0302	0.100	—	—	0.00842	—	—
		II	0.0510	0.1490	1.11	1.61	0.00372	—	—
		III	0.0465	0.1310	—	—	0.00312	0.142	0.0460
4	1	I	0.0187	0.0430	—	—	0.00789	—	—
		II	0.0355	0.0713	1.39	5.01	0.00675	—	—
		III	0.0320	0.0668	—	—	0.00650	0.261	0.0454
	2	I	0.0239	0.0675	—	—	0.00748	—	—
		II	0.0301	0.0718	0.631	17.1†	0.00446	—	—
		III	0.0326	0.0748	—	—	0.00392	0.310	0.0257
5	1	I	0.0203	0.0443	—	—	0.0116	—	—
		II	0.0408	0.0697	1.78	1.63	0.00502	—	—
		III	0.0363	0.0602	—	—	0.00285	0.203	0.0600
6	1	I	0.0193	0.0633	—	—	0.0130	—	—
		II	0.0450	0.120	1.25	0.895	0.00392	—	—
		III	0.0440	0.1160	—	—	0.00386	0.0620	0.0542
	2	I	0.0271	0.0929	—	—	0.00347	—	—
		II	0.0299	0.1070	0.269	29.6†	0.00425	—	—
		III	0.0273	0.1010	—	—	0.00353	0.267	0.0093
7	1	I	0.0376	0.125	—	—	0.01150	—	—
		II	0.0610	0.172	1.18	0.767	0.00429	—	—
		III	0.0600	0.167	—	—	0.00420	0.0672	0.0698
	2	I	0.0275	0.1220	—	—	0.00591	—	—
		II	0.0358	0.1620	0.473	9.19†	0.00649	—	—
		III	0.0340	0.1410	—	—	0.00611	0.176	0.0164
8	1	I	0.0411	0.0623	—	—	0.0157	—	—
		II	0.0674	0.0776	1.51	3.13	0.00502	—	—
		III	0.0673	0.0769	—	—	0.00500	0.319	0.1027
	2	I	0.0297	0.0755	—	—	0.00620	—	—
		II	0.0468	0.1010	0.735	7.63†	0.00400	—	—
		III	0.0450	0.0968	—	—	0.00379	0.284	0.0306
9	1	I	0.0696	0.1180	—	—	0.0155	—	—
		II	0.115	0.1300	1.25	1.49	0.00278	—	—
		III	0.115	0.1300	—	—	0.00278	0.212	0.1430
10	1	I	0.0269	0.0663	—	—	0.0126	—	—
		II	0.0476	0.0959	1.51	2.03	0.00430	—	—
		III	0.0466	0.0937	—	—	0.00428	0.161	0.683

* The logarithmic coefficient of variation, as defined in text. For all symbols, see text. Dashes indicate that parameter is not appropriate for the model.

† In these runs the coronary circulation was maximally dilated. The values for τ_{em} are physically impossible.

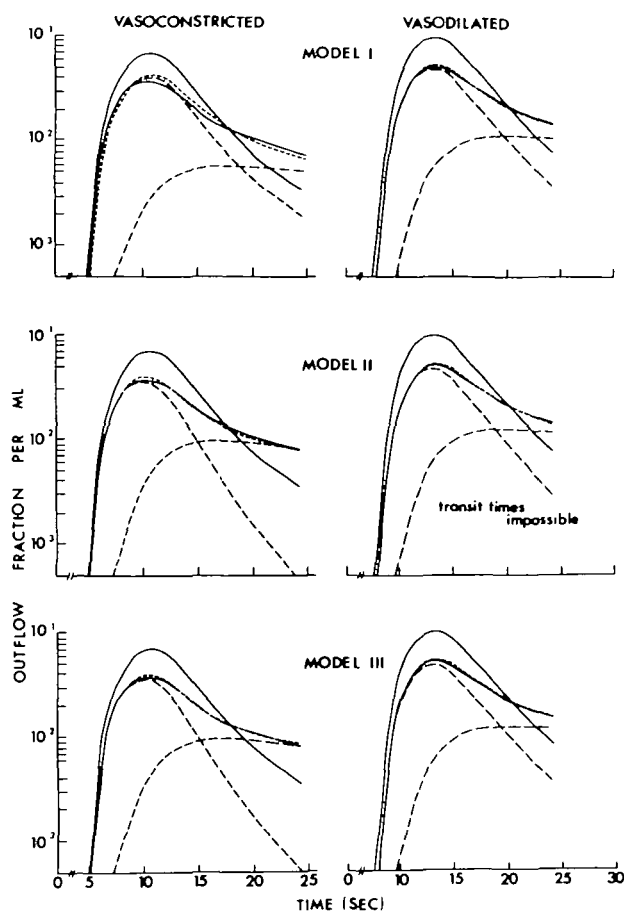


FIGURE 4 Examples of the results of fitting the three models to the data from the two runs of the first experiment in Table 1. The upper solid line is the normalized output of the intravascular reference (^{125}I -albumin), and the lower solid line, that for the diffusible tracer (^{14}C -sucrose). The latter crosses over the former as the diffusible tracer returns from the extravascular space. The model curve fits to the diffusible tracer are displayed in terms of their two components: the first or throughput component, the diffusible tracer which has not left the capillary, is displayed by means of long-dashed lines; and the later component, the tracer which has returned from the extracellular space, is also outlined by long-dashed lines. The total, the sum of the two components, is represented by a short-dashed line. In the upper left panel the short-dashed line on the upslope represents both the throughput and the total.

almost as well as model III, the values of the parameters obtained with the fit appear reasonable. However, in the experiments in which the preparation has been vasodilated, when the fit with model II is relatively poor, physically unacceptable values for τ_{cm} are found.

Compared to model III, model I (the constant capillary transit time model) tends to underestimate the value for k_a and model II (the constant large vessel transit time model), to overestimate it.

Figure 5 shows the effect of correction for catheter distortion¹⁴ on the log ratio-time curve. There is no significant change in the form of the curve. We have found that fitting the same models to the catheter-corrected data generally results in a slightly larger value for τ_{cm} but that the value for k_a remains the same. We therefore have not pursued this matter.

It is also worth commenting on the results of the analysis of the example experiment (experiment 1) displayed in Figure 2. While the initial guess for b' in run 2 (the fibrillating, maximally dilated case) was close to zero, the final value for b' , coming from the fit to the whole curve, is a small positive value. This indicates that there is a small dispersion of capillary transit times, even in the maximally vasodilated case. It is also appropriate to note that the experimental error (and the scatter) in the ratio values will be largest for the lowest values on the upslopes of the dilution curves.

Discussion

THE UTILITY OF THE PRESENT MODELING

Much of the model analysis of dilution curves from the heart has been carried out on the basis of the assumption that for each capillary there is a single common transit time.^{1, 3, 8, 7, 11, 12} As a result of this, a common expectation has evolved that a value for extraction, $1 - [C(t)_{diff} / C(t)_{ref}]$, could be determined from the early values of the curves, that this would probably be constant over several samples, and that it would be representative of the whole organ. Alvarez and Yudilevich,⁵ indeed, did find constant extraction values in their early samples, in data obtained from isolated hearts. However, in intact functioning hearts, Ziegler and Goresky^{6, 13} and Downey and Kirk¹⁴ have found increasing values for early extractions, and, indeed, the observations in the present study conform to this same pattern, apart from the vasodilated or fibrillating heart. It is appropriate to note that, unlike Alvarez and Yudilevich,⁵ Guller et al.¹² did observe increasing early extractions of labeled sodium in multiple indicator-dilution studies carried out in an isolated perfused nonworking heart, although the phenomenon was much smaller in magnitude than it is in the intact heart in situ. These authors noted the phenomenon, suggested that it was due to heterogeneity of perfusion, and pointed out that their modeling had not yet been extended to include this; then they suggested that peak or maximal extractions were, in any case, representative of the whole and could be used, with a suitable empirical correction, to derive values for the permeability.

Our model analysis indicates that the problem is more complex than these considerations have indicated, that the phenomenon is important, and that there is no one extraction that is representative except in the case of maximal vasodilation. The presence of constant extractions in the isolated preparations of Alvarez and Yudilevich⁵ is probably due to the use of perfusion media of low oxygen-carrying capacity (that is, to the ensuing vasodilation), as well as to the lack of either a ventricular pressure gradient or intact neural pathways, in this preparation. Thus the single transit time (or constant extraction) model, equivalent to model I, which has been used in all previous analyses, is useful in the heart only as an asymptotic approximation in a preparation in which there is maximal vasodilation. Here it is approximately valid.

While it is obvious that vasodilation reduces capillary transit time heterogeneity, it is not possible, using sucrose as the permeable tracer, to derive a parameter from model III

TABLE 3 Data for First Experiment of Table 1

Sample	Time (sec)	10 ⁶ × outflow fraction per ml			
		Run 1		Run 2	
		¹²⁵ I-Albumin	¹⁴ C-Sucrose	¹²⁵ I-Albumin	¹⁴ C-Sucrose
10	7.50	4,659	3,462	0	0
11	8.25	14,349	10,069	0	0
12	9.00	27,000	18,065	0	0
13	9.75	39,988	26,096	1,336	668
14	10.50	53,106	32,598	8,004	4,042
15	11.25	64,169	36,850	23,844	12,196
16	12.00	67,491	36,516	45,043	22,493
17	12.75	69,268	36,692	68,100	34,355
18	13.50	64,396	34,671	89,289	43,528
19	14.25	58,296	31,367	97,471	49,784
20	15.00	48,592	27,660	102,216	51,471
21	15.75	39,388	24,321	96,558	50,188
22	16.50	32,000	20,578	91,503	47,394
23	17.25	24,776	16,747	73,264	41,771
24	18.00	20,594	15,833	61,142	37,219
25	18.75	16,958	14,000	50,000	34,000
26	19.50	13,513	13,513	41,938	30,000
27	20.25	11,617	12,301	35,452	27,448
28	21.00	9,531	11,704	27,839	23,302
29	21.75	7,800	10,900	23,339	21,931
30	22.50	6,540	10,368	19,303	20,718
31	23.25	5,895	9,876	14,922	18,500
32	24.00	5,236	9,130	13,317	17,397
33	24.75	4,668	8,628	10,786	16,500
34	25.50	3,932	8,242	9,689	15,587
35	26.25	3,500	7,838	7,981	14,744

which unambiguously represents transit time heterogeneity and which can be compared in different preparations. The value for b' in Table 2 varies with k_s and γ as well as the heterogeneity. While k_s can be found, γ is indeterminate in model III. Thus while b' decreases with vasodilation we cannot calculate the absolute values for b . It could be argued that this change in transit time heterogeneity was due to a decrease in the perfusion pressure at constant flow. However, a reduction in the perfusion pressure, all else being equal, could be expected only to increase the heterogeneity and not to decrease it.

For sucrose, a tracer with a low permeability, model I results in an estimate of permeability which is lower, by a factor of no more than 2, in the vasoconstricted situation than the estimate arising from model III, the best fitting model. This underestimate will be expected to be greater for tracers with higher permeabilities, because model I grossly underestimates the amount of material returning from the extravascular space early in time. Thus, when the tracers being used have a high permeability and where their proportionate return is large, early in time, the error with the single capillary transit time model will be even larger.

A check on the overall validity of the modeling can be made by comparing the estimate of the total accessible sucrose space to other measurements of the extracellular space. We know from previous⁶ model-independent calculations (from dilution studies in which virtually complete labeled sucrose and albumin curves were recorded, in the absence of recirculation, so that accurate experimental

values for the mean transit times for the two substances could be obtained) that the accessible extravascular space for sucrose is 0.084 ml/g or slightly higher. Model II in the nonvasodilated preparations gives a value for γ of about 1.2. Thus the intravascular space for sucrose is $0.084/1.2 = 0.070$ ml/g and the total space is 0.154 ml/g. Polimeni¹⁶ has used morphometric and equilibrative tracer techniques to measure total extracellular space in the rat heart. He reports values of about 0.19 ml/ml for the rat ventricle. Since, for the vasoconstricted case, there are probably some unperfused capillaries, γ is larger than if all capillaries were perfused; hence one would expect to underestimate the size of the total extracellular space measured after equilibration. The agreement between the estimates of Polimeni and those coming from the present study thus appears very good.

We therefore believe that, despite the simplifying assumptions used, model III is a very good approximation to the behavior of the coronary microcirculation. It is also appropriate to emphasize that when the preparation is quite vasoconstricted, its behavior closely approaches the asymptotic model II. The parameters derived from the analysis of the dilution curves with model II in the vasoconstricted case can also be used to calculate capillary permeability for sucrose. If rad is the radius of a capillary, L is the length of a capillary, and Hct is the capillary hematocrit, the product $k_s\gamma = 2P \cdot radL / (\pi rad^2 L [1 - Hct]) = 2P / (rad [1 - Hct])$. Thus if we know $k_s\gamma$ and rad , we can approximate P , independent of any assumptions about capillary surface. In the present study we have found that $k_s\gamma$ varies from 0.05

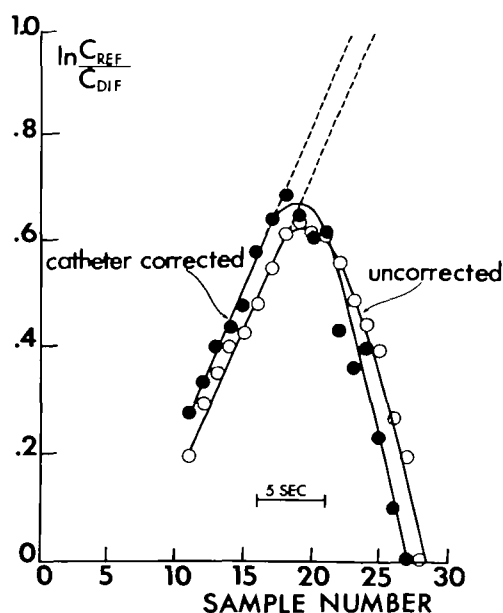


FIGURE 5 Effect of correction for catheter distortion on the log-ratio time plot. We have not shown the effect of correction of the appearance time since this is essentially irrelevant to the fitting procedure. It would only reduce the appearance time for all tracers equally.

sec^{-1} to 0.14 sec^{-1} . Bassingthwaighe et al.¹⁷ report capillary radii averaging $2.8 \mu\text{m}$. If the average value of the hematocrit is 0.40, P has a range of 2.2 to $3.3 \times 10^{-8} \text{ cm/sec}$.

VARIATION OF DERIVED PARAMETERS WITH FLOW

Previous investigators using relatively vasodilated preparations^{8, 9, 18} have found that the permeability-surface product increases with increasing flow and have attributed this to recruitment. This is to be expected in a passive system in which the increase in pressure accompanying the increase in flow will force open more capillaries. In an autoregulating preparation no such simple correlation will be expected. In the present set of experiments we took the option of controlling the flow so that it would not, of itself, produce changes in the distribution of perfusion; and, after a first run, carried out a second experiment at the same flow, in the presence of a stimulus causing coronary vasodilation. Although this was suitable for the purposes for which the current experiments were designed, it does not correspond to the usual *in vivo* situation. There, when flow is increased, the resistance vessels will tend to constrict, further reducing the number of open capillaries. In Figure 6 we show results of an experiment illustrating the changes in shape of dilution curves in this other kind of situation, where flow has been deliberately increased, but the coronary circulation is allowed to autoregulate. At the low flow the maximal extraction is near the peak, but at the higher flow the maximal extraction is found at a time when the reference tracer has assumed a value less than 10% of peak. Even though the maximal extractions are comparable, the proportionate contribution of the returning component to the sucrose dilution curve, early in time, has been markedly reduced in

the high flow experiment. This kind of shape change was found early in our exploration of the heterogeneity phenomenon, before we settled out on our final experimental design (and, as a consequence, these experiments are not reported here). The shape change was found to occur consistently (it is the converse of that illustrated in Figure 1), and further emphasizes the futility of attempting to define a single representative extraction.

THE THEORETICAL BASIS OF THE PARALLEL CAPILLARY-LARGE VESSEL UNIT MODEL

Thus, from our experimental data, we have inferred that maximal vasodilation is associated with a constant capillary transit time and that vasoconstriction causes an increase in the heterogeneity of the transit times. We believe that this phenomenon can be explained by examining the flow patterns to be expected in a capillary network fed by a varying number of precapillary sphincters.

We assume that the basic unit of the coronary microcirculation is a capillary network fed by a single arteriole and drained by a single venule. Most of the network is composed of long parallel capillaries but these are joined at random intervals by anastomoses. The lengths of the large vessels leading to and away from the network are fixed for each network but differ in different networks. The input to the network is controlled by precapillary sphincters. When all the sphincters are open (maximal vasodilation), there will be little or no tendency for blood to flow through the anastomoses between the major capillaries, since the intravascular pressure will be equal at each point along the capillaries. If the major capillaries are of equal length, then their transit times will be equal. When only a fraction of the sphincters leading to the network are open, the pressure differences between the major capillaries are variable and the path length in any given net will depend both upon which sphincters are open and upon the detailed structure of the network. In Figure 7 we have attempted to illustrate in two dimensions this change from vasodilated to vasoconstricted, for two different hypothetical networks. We have shown the sphincters to be either fully open or closed but the real situation is probably more complicated than this.

There is also undoubtedly control of total flow through the networks by the arteriolar sphincters but this cannot be

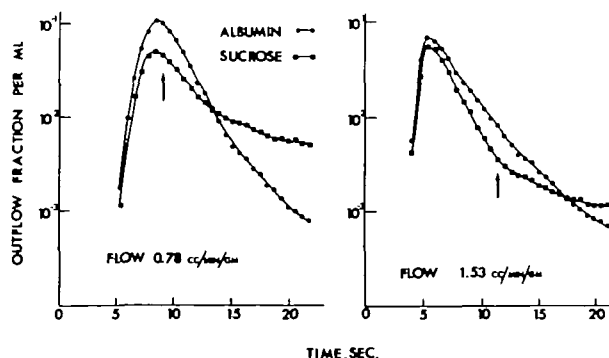


FIGURE 6 Effect of increased flow on the dilution curves, when the coronary circulation is allowed to autoregulate. Arrows indicate the time at which maximal extraction occurs.

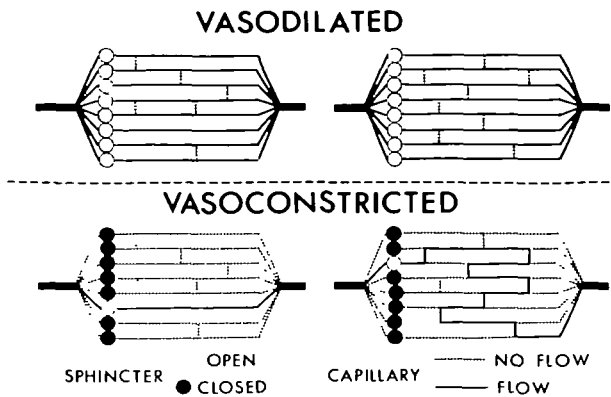


FIGURE 7 Highly schematic diagram of two theoretical capillary-large vessel units differing greatly in the degree of vasomotor tone. In the vasodilated unit, pressures along each capillary are equal and there is no flow through anastomoses, whereas in the vasoconstricted unit flow will tend to be more or less random in the network. The panel at the lower right shows some reversal of direction of flow. This was necessary in order to compress the actual three-dimensional network into two dimensions. We have never observed precession of a diffusible indicator on the intravascular reference. This would have been observed if there were significant counterflow.

the major influence on the heterogeneity of capillary transit times. Vasoconstriction results in capillary transit times much shorter than the average, as well as much longer. Constriction of an arteriolar sphincter at constant total flow could not cause a decrease in transit time within a unit, only an increase. This can occur only if there are statistically shorter pathways through the network. Thus what we see experimentally as a heterogeneity of capillary transit times appears to result mostly from the selection of pathways through the capillary network rather than from changes in flow, mediated by adjustments at the level of the arteriole. The degree of heterogeneity detected by the microsphere injection and I-g tissue sampling studies (14% of average flow) appears to be incapable of explaining the great range of capillary transit times inferred from the present study. The transit time heterogeneity appears to be occurring at a more microscopic level.

In the vasoconstricted state the total transit time through each unit will be determined to a greater extent by the capillary transit time, and the fixed differences in large vessel lengths will become less important. So far we have found only one run (experiment 9, Table 1) in the heart in which the large vessel transit times appear to become constant, i.e., in which model II fits as well as model III. This probably is due to the anatomical limitations imposed by the supplying and draining large vessels. Blood can be supplied to the mammalian myocardium only from the epicardial surface by penetrating vessels of various lengths. The patterns in other organs differ. The liver and the lung have a lobular structure, and analysis of indicator-dilution data from these indicates that the large vessel transit times are relatively uniform, and that the pattern of distribution corresponds closely to model II.^{4, 10}

What we have said so far may seem hypothetical but there is more or less direct proof from the indicator-dilution data itself. The linear relation between capillary transit time and

elapsed time which has been found to fit every experiment appears to depend on the presence of a system composed of parallel pathways of coupled capillaries and large vessels (that is, a system in which both reduced flow along the appropriate large vessel transit pathway leads to reduced flow in the particular capillaries supplied, and increased flow along the one leads to increased flow in the other). If capillaries with identical transit times were connected to large vessel pathways of greatly different transit times, experimental elapsed time would not arrange the capillary transit times in order of increasing transit time but in some more or less random order. Thus, except in the case of constant capillary transit times (model I), the whole organ impulse response of the coronary circulation is not a convolution of capillary and large vessel transit time distributions as Bassingthwaite⁹ has proposed, but instead is an arrangement of discrete parallel pathways. Hence, each sample collected at the output after the appearance time potentially represents the output from a single type of capillary-large vessel unit. Strictly, this would be true only if samples could be collected infinitely rapidly. However, it can be taken to be approximately true for samples of short but finite duration. Thus a given increment in experimental time will correspond to a constant increment in capillary transit time. The increment in transit time will depend upon the degree of heterogeneity of transit times relative to the shortest one. If there is no heterogeneity, the increment will

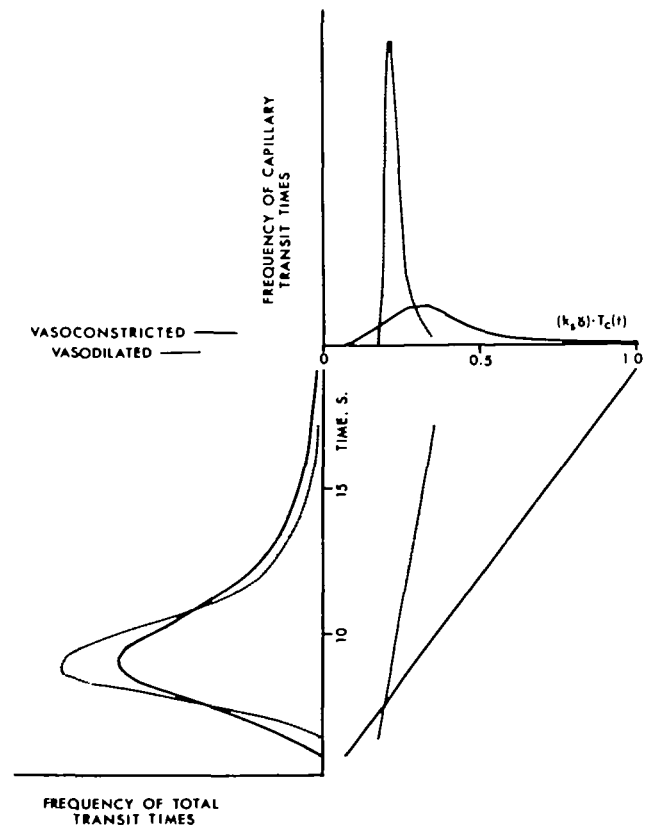


FIGURE 8 Effect of changes in vascular resistance on the frequencies of total transit times and capillary transit times. See text for explanation.

be zero (model I); whereas, if there is heterogeneity, the increment will be proportional to the degree of vasoconstriction. If the dispersion becomes great enough and samples could be collected fast enough, the dilution curves would be expected to be quantized into pulses of progressively increasing transit times, representing the output from individual units. In other words, the deduced phenomenon of a linear relation between capillary transit time and elapsed experimental time is a macroscopic manifestation of the quantum nature of microcirculatory transport.

So far we have considered the behavior of types of parallel pathways and not the frequency of each type. In Figure 8 we have used data from experiment 7 to illustrate how the frequency of capillary transit times changes with vascular resistance. The dilution curves for the intravascular reference are shown at the bottom left. The areas of the curves are equal and therefore give the relative frequency of total transit times through the microcirculation. According to our analysis the total transit time for any elapsed experimental time is the sum of a unique capillary transit time and a coupled large vessel transit time. The capillary transit times are related to elapsed time by Equation 9. Since $k_p \gamma = 2P/(\text{rad}[1 - \text{Hct}])$ is constant in the same preparation, the abscissa of the upper panel of Figure 8 is proportional to the capillary transit time. The relative frequency of capillary transit times can then be obtained from the frequency of total transit times by equalizing the areas in the upper panel. We have assumed that the spectrum of capillary transit times in the vasoconstricted state is equal to the spectrum of total transit times, since model II fits almost as well as model III for this experiment. Note that the small change with vascular resistance in the frequency of total transit times is magnified when the dispersion of large vessel transit times is factored out. The reduction in mean capillary transit time with vasodilation is probably due to a reduction in capillary volume secondary to the reduction in perfusion pressure at constant flow. This is reflected in the reduction of k_p from 0.06 to 0.034 sec⁻¹.

There is additional evidence from two other areas that vasomotor activity in the coronary circulation is not just a flow-regulating system but is also associated with profound changes in the flow patterns in the microcirculation. The microsphere injection, tissue sampling studies also suggest that maximal vasodilation abolishes perfusion heterogeneity.⁹ Also Bourdeau-Martini et al.²⁰ have shown that the distribution of intercapillary distances is sensitive to the PO₂ of the perfusing blood. During hypoxia, which is presumably associated with vasodilation, the distribution becomes more uniform than in the normal or mildly hyperoxic situation. These data are certainly consistent with our hypothesis. Our analysis, however, emphasizes that transport is more dependent on the transit time distribution of the organ than on intercapillary distances. The reason for the existence of a mechanism for controlling this distribution is unknown. While it may be a secondary effect of the flow controlling mechanism, it may also be a mechanism for optimizing oxygen transport.

The presence of a heterogeneity of capillary transit times is also substantiated by the work of Monroe et al.,²¹ who have found a very large heterogeneity in the oxygen saturation of blood in small coronary veins. They found that the heterogeneity almost disappears when vasodilation is induced. The change with vasodilation appears to rule out the possibility that the heterogeneity resides in local patterns of oxygen consumption. Thus, even for highly diffusible substances like oxygen, there is probably very little diffusional shunting between unlike capillary-large vessel units, and the main determinant of extraction is the transit time within each unit.

Acknowledgments

We thank Dr. Glen G. Bach for his helpful conversations, Denise Joubert, Louise Gagnon, and Kim McMillan for their technical assistance; and Margaret Mulhern for typing this manuscript. The flavaspidic acid was a gift from Dr. Esa Aho of Huhtamäki-yhtymä Oy, Helsinki, Finland

References

- Goresky CA, Ziegler WH, Bach GG: Capillary exchange modeling, barrier-limited and flow-limited distribution. *Circ Res* 27: 739-764, 1970
- Perl W, Chinard FP: Convection-diffusion model of indicator transport through an organ. *Circ Res* 22: 273-298, 1968
- Bassingthwaight JB, Knopp TJ, Hazelrig JB: A concurrent flow model for capillary-tissue exchanges. In *Capillary Permeability*, edited by C Crone and NA Lassen. Copenhagen, Munksgaard, 1970, pp 60-80
- Goresky CA: A linear method for determining liver sinusoidal and extravascular volumes. *Am J Physiol* 204: 626-640, 1963
- Alvarez OA, Yudilevich DL: Heart capillary permeability to lipid-insoluble molecules. *J Physiol (Lond)* 202: 45-58, 1969
- Ziegler WH, Goresky CA: Transcapillary exchange in the working left ventricle of the dog. *Circ Res* 24: 181-207, 1971
- Bassingthwaight JB: A concurrent model for extraction during transcapillary passage. *Circ Res* 35: 483-503, 1974
- Falsetti HL, Carroll RJ, Marcus ML: Temporal heterogeneity of myocardial blood flow in anesthetized dogs. *Circulation* 52: 848-853, 1975
- Sestier F, Mildenberger R, Klassen G: Cyclic changes in coronary flow: a consequence of autoregulation (abstr). *Circulation* 52 (suppl 2): 126, 1975
- Chinard FP, Vosburgh GJ, Enns T: Transcapillary exchange of water and other substances in certain organs of the dog. *Am J Physiol* 183: 221-234, 1955
- Crone C: Permeability of capillaries in various organs as determined by the "indicator diffusion" method. *Acta Physiol Scand* 58: 292-305, 1963
- Guller B, Yipintsoi T, Orvis AL, Bassingthwaight JB: Myocardial sodium extraction at varied coronary flows in the dog: estimation of capillary permeability by residue and outflow detection. *Circ Res* 37: 359-378, 1975
- Ziegler WH, Goresky CA: Kinetics of rubidium uptake in the working dog heart. *Circ Res* 24: 208-220, 1971
- Goresky CA, Silverman M: Effect of correction of catheter distortion on calculated liver sinusoidal volumes. *Am J Physiol* 207: 883-892, 1964
- Downey HF, Kirk ES: Indications from coronary lymph and early extraction data that steady state uptake of ⁴²K is not primarily limited by the capillary wall. In *Capillary Permeability*, edited by C Crone and NA Lassen. Copenhagen, Munksgaard, 1970, pp 326-340
- Polimeni PI: Extracellular space and ionic distribution in rat ventricle. *Am J Physiol* 227: 676-683, 1974
- Bassingthwaight JB, Yipintsoi T, Harvey RB: Microvasculature of the dog left ventricle myocardium. *Microvasc Res* 7: 229-249, 1974
- Yipintsoi T, Tancredi R, Richmond D, Bassingthwaight JB: Myocardial extractions of sucrose, glucose, and potassium. In *Capillary Permeability*, edited by C Crone and NA Lassen. Copenhagen, Munksgaard, 1970, pp 153-156
- Goresky CA, Cronin RFP, Wangel BE: Indicator dilution measurements of extravascular water in the lungs. *J Clin Invest* 48: 487-501, 1969
- Bourdeau-Martini J, Odoroff CL, Honig CR: Dual effect of oxygen on magnitude and uniformity of coronary intercapillary distance. *Am J Physiol* 226: 800-810, 1974
- Monroe RG, Gamble WJ, LaFarge CG, Benoualid H, Weisul J: Transmural coronary venous O₂ saturations in normal and isolated hearts. *Am J Physiol* 228: 318-324, 1975